HYDROLOGICAL PROCESSES
Hydrol. Process. **22**, 1588–1603 (2008)
Published online 30 July 2007 in Wiley InterScience
(www.interscience.wiley.com) DOI: 10.1002/hyp.6728

The influence of elevation error on the morphometrics of channel networks extracted from DEMs and the implications for hydrological modelling

John B. Lindsay* and Martin G. Evans
Upland Environments Research Unit (UpERU), School of Environment and Development, University of Manchester, Oxford Road, Manchester M13 9PL, UK

Abstract:

Stream network morphometrics have been used frequently in environmental applications and are embedded in several hydrological models. This is because channel network geometry partly controls the runoff response of a basin. Network indices are often measured from channels that are mapped from digital elevation models (DEMs) using automated procedures. Simulations were used in this paper to study the influence of elevation error on the reliability of estimates of several common morphometrics, including stream order, the bifurcation, length, area and slope ratios, stream magnitude, network diameter, the flood magnitude and timing parameters of the geomorphological instantaneous unit hydrograph (GIUH) and the network width function. DEMs of three UK basins, ranging from high to low relief, were used for the analyses. The findings showed that moderate elevation error (RMSE of 1·8 m) can result in significant uncertainty in DEM-mapped network morphometrics and that this uncertainty can be expressed in complex ways. For example, estimates of the bifurcation, length and area ratios and the flood magnitude and timing parameters of the GIUH each displayed multimodal frequency distributions, i.e. two or more estimated values were highly likely. Furthermore, these preferential estimates were wide ranging relative to the ranges typically observed for these indices. The wide-ranging estimates of the two GIUH parameters represented significant uncertainty in the shape of the unit hydrograph. Stream magnitude, network diameter and the network width function were found to be highly sensitive to elevation error because of the difficulty in mapping low-magnitude links. Uncertainties in the width function were found to increase with distance from outlet, implying that hydrological models that use network width contain greater uncertainty in the shape of the falling limb of the hydrograph. In light of these findings, care should be exercised when interpreting the results of analyses based on DEM-mapped stream networks. Copyright © 2007 John Wiley & Sons, Ltd.

KEY WORDS drainage network indices; morphometrics; hydrological modelling; error modelling; digital elevation models

Received 11 August 2006; Accepted 26 February 2007

INTRODUCTION

For larger basins, the flood hydrograph is heavily influenced by the stream residence time, which is itself partly influenced by the geometric structure of the drainage network. This fact has largely been the motivation behind the development of indices of drainage network geometry, or network morphometrics (Wharton, 1994). Several hydrological models take advantage of the link between network form and runoff response by using morphometrics. The geomorphological instantaneous unit hydrograph (GIUH) (Rodriguez–Iturbe and Valdes, 1979) and the network width function (Mesa and Mifflin, 1986; Naden, 1992) are two related and common examples of models that relate properties of a basin's stream network to runoff response. These models have been used extensively as they generally provide satisfactory results and because, aside from channel network data which is readily available, they require few parameters (Beven, 2000).

Although there is substantial potential for using morphometrics for hydrological modelling, accurate stream mapping remains one of the greatest challenges for further development. Manual stream mapping is a highly subjective practice; different cartographers can produce very different stream networks (Mark, 1984). Several algorithms exist for extracting drainage features from digital elevation models (DEMs), each of which offer the advantage of being more efficient and reproducible than manual mapping (for a recent review see Heine *et al.*, 2004). Thus, DEM-based stream mapping is widely used for hydrological applications. It is important, however, to quantify the uncertainty associated with automated extraction of drainage networks from DEMs as it is a potentially significant source of error in the applications of these data. Several researchers have recently stressed the importance of uncertainty analysis in hydrological and geomorphological modelling (e.g. Wolock and Price, 1994; Gyasi–Agyei *et al.*, 1995; Walker and Willgoose, 1999; Endreny *et al.*, 2000; Kenward *et al.*, 2000; Endreny and Wood, 2001).

The error in automated channel mapping is associated with (1) algorithm design and implementation; (2) parameterization (e.g. selection of threshold values);

* Correspondence to: John B. Lindsay, School of Environment and Development, Mansfield Cooper Building, University of Manchester, Oxford Road, Manchester M13 9PL, UK.
E-mail: John.Lindsay@manchester.ac.uk

and (3) error in the DEM. Tribe (1992) showed how different channel mapping algorithms could provide significantly different results. Gandolfi and Bischetti (1997) and Da Ros and Borga (1997) also demonstrated that drainage network indices, and the form of the GIUH and width function, are sensitive to the contributing area threshold, a parameter used to identify channel heads. DEM error, however, is perhaps the most basic source of uncertainty in channel mapping. Specifically, these errors result from the tessellation of Earth's surface (McMaster, 2002) and elevation error (Lee *et al.*, 1992). The first issue is perhaps less important now than it was in the past, as fine-resolution DEMs become increasingly accessible to hydrologists. In contrast, elevation error continues to be problematic because relatively little is known about the nature and propagation of this error source (Carlisle and Heywood, 1996). It is currently unknown to what extent elevation error influences the geometric properties of drainage networks extracted from DEMs. Consequently, the uncertainties in runoff models that are based on network morphometrics are also unknown. We address these issues by asking: how does elevation error influence the reliability of the estimates of the geometry of extracted drainage networks and the uncertainty in the GIUH and width function?

BACKGROUND

Network morphometrics and morphometrics-based runoff models

Numerous drainage network indices have been developed with the intention of describing variations in and evolution of network form, quantifying the effects of environmental controls on the fluvial system and identifying the influence of network geometry on hydrological response (Knighton, 1998). Several network morphometrics are based on the stream ordering system developed by Horton (1945) and later modified by Strahler (1952). Most notable among these indices are the so-called *laws of drainage network composition*, which state that when plotted against stream order, the number of streams, average length, average drainage area and average channel slope approximate geometric series (Horton, 1945; Schumm, 1956). These relations are summarized for a stream network using the bifurcation R_B, length R_L, area R_A and slope R_S ratios, which are often referred to as Horton ratios. These four network indices have relatively narrow ranges, suggesting that there is either regularity in the structure of rivers or insensitivity in the Horton–Strahler ordering scheme to natural variation. Drainage density is another index of hydrological significance that was suggested by Horton (1932; 1945). Defined as the total stream length divided by basin area, drainage density is a measure of the extent to which a basin is dissected by rivers, and is therefore commonly used to describe drainage efficiency.

Link magnitude M and network diameter D are two important topological indices of drainage networks, which have been used in the probabilistic-topologic approach to network analysis (Shreve, 1966; Werner and Smart, 1973; Smart, 1978). M is defined as the number of source channels flowing to a particular link within a drainage network. As with stream order, M is a topological measure of the position of a reach within the overall network structure. D is the maximum network link distance and is a topological description of the extent of a drainage network.

Morphometrics are used to model the network response function in both the GIUH (Rodriguez–Iturbe and Valdes, 1979) and network width function (Kirkby, 1976) approaches to rainfall–runoff modelling. Based on GIUH theory, the various links in a drainage network can be viewed as a series of cascading reservoirs with varying residence times. The original formulation of the GIUH was described in the classic paper by Rodriguez–Iturbe and Valdes (1979). Based on their work, the two most important parameters for defining the shape of the unit hydrograph are the peak flow q_p and the time to peak t_p, defined respectively as:

$$q_p = \theta v \tag{1}$$

$$t_p = k \Big/ v \tag{2}$$

where v is the mean stream flow velocity and θ and k characterize geomorphological control on runoff. θ and k are calculated using Horton ratios, such that:

$$\theta = \frac{1{\cdot}31}{L_\Omega} R_L^{0{\cdot}43} \tag{3}$$

$$k = 0{\cdot}44 L_\Omega \left(\frac{R_B}{R_A}\right)^{0{\cdot}55} R_L^{-0{\cdot}38} \tag{4}$$

where L_Ω is the length of the highest order stream measured in kilometres, and serves as a scaling parameter.

Kirkby (1976) defined the network width function $N(x)$ as the number of links at successive distances x from the basin outlet. Thus, as with M and D, $N(x)$ describes network structure using a topological representation. $N(x)$ has been utilized for hydrological modelling, based on the notion that the relative importance of the hillslope response function diminishes for larger basins and the overall response is increasingly dominated by holding times within the channel network (Kirkby, 1976; Gupta and Messa, 1988). Although related to the GIUH, it has been argued that $N(x)$ is potentially more useful for hydrological prediction because, unlike Horton ratios, it explicitly describes the spatial distribution of streams within a basin (Knighton, 1998; Gandolfi *et al.*, 1999). Surkan (1969) showed that $N(x)$ could be directly related to the unit hydrograph and the runoff routing response. Similarly, Naden (1992) used $N(x)$, as well as velocity and dispersion parameters, as a transfer function for hydrograph prediction.

Monte Carlo approaches to the study of error propagation

Stochastic simulation, or the Monte Carlo method, has been widely used to assess uncertainty in data derived

DOI: 10.1002/hyp

from DEMs because many terrain analysis functions are too complex for analytical approaches (e.g. Hunter and Goodchild, 1997; Burrough and McDonnell, 1998; Fisher, 1998). The technique has been used in the past to study uncertainty in DEM-extracted stream networks (Lee *et al*., 1992; Gatziolis and Fried, 2004; Lindsay, 2006), although it has never been used to examine uncertainty in network geometric properties. Stochastic simulation is a brute force technique that is extremely computationally demanding. The assumptions of the technique, as applied to error propagation study in the field of terrain analysis, are: (1) DEM error exists and constitutes uncertainty that is propagated with the manipulation of terrain data; (2) the exact nature of these errors is unknown; (3) DEM error can be represented by a distribution of topographic realizations; and (4) the true surface lies somewhere within this distribution of surfaces (Wechsler, 2000).

In general, a stochastic simulation operates as follows. First, error distributions are assigned to each grid cell of the DEM. An error field is then generated by drawing a random sample from the individual grid cell error distributions. This error field can then be added to the DEM to create a new terrain realization. Data are extracted from the new DEM (e.g. a stream network and its geometric properties) and the above procedure is repeated iteratively until a stopping condition is met. An alternative, equally probable realization of the extracted information is created with each iteration of the procedure. A frequency distribution of the extracted information is built up over the course of the simulation. The characteristics of this frequency distribution can then be used to make inferences about the effects of DEM error on the reliability of the extracted information.

In generating error fields for a simulation, it is important to consider the statistical distribution of error as well as the spatial properties of elevation error (Fisher, 1998). Spatial properties of error include the degree of autocorrelation and the distance of dependency, i.e. the distance beyond which two points are unlikely to be correlated. The spatial aspects of error fields are often evaluated using a semi-variogram (Burrough and McDonnell, 1998).

When information about the statistical and spatial distribution of error in a DEM is available, these data may be used as a basis for generating error fields in a conditional simulation (Heuvelink, 1998; Carr, 2002). This empirical approach to error field generation requires higher accuracy reference data, from which the spatial properties of elevation error are derived (Wechsler, 2006). When these data are either unavailable or too costly to obtain, as is often the case, assumptions must be made about the nature of error based on heuristics rather than empirical analysis (Oksanen and Sarjakoski, 2005; Wechsler, 2006). One common assumption is that the statistical distribution of error is Gaussian with a mean of zero and a standard deviation equal to the root-mean-square error (RMSE), a frequently published measure of DEM error (Gatziolis and Fried, 2004). The second common assumption made in heuristic approaches to error propagation study is that DEM error possesses some degree of spatial autocorrelation (Wechsler, 2006). While empirical approaches to error analysis typically derive the spatial properties of error using a higher accuracy reference data set, heuristic approaches often present results for a series of simulations with error fields possessing a range of spatial properties (e.g. Gatziolis and Fried, 2004; Lindsay, 2006). This compensates for the often unknown spatial characteristics of error.

At least four different techniques have been commonly adopted to generate random fields with specified degrees of spatial autocorrelation for use in error modelling, including: (1) simulated annealing or pixel swapping (Fisher, 1991; Deutsch and Journel, 1998); (2) spatially autoregressive models (Goodchild *et al*., 1992); (3) spatial moving averages using low-pass filters (Wechsler, 2000; Cressie and Pavlicová, 2002; Gatziolis and Fried, 2004; Oksanen and Sarjakoski, 2005); and (4) sequential Gaussian simulation (Goovaerts, 1997; Deutsch and Journel, 1998). Oksanen (2006) and Wechsler (2006) both provide useful reviews of these techniques in the context of error modelling for terrain analysis. Each of the techniques for generating error fields has various advantages and disadvantages that affect their suitability for certain applications.

The spatial moving averages (SMA) approach is very attractive for error propagation modelling because it is not as computationally demanding as other techniques, meaning that numerous realizations can be achieved even for large grids (Oksanen and Sarjakoski, 2005). This is important because the traditional use of a small number of realizations (<100) that is common with more computationally demanding techniques, such as sequential Gaussian simulation, can result in non-convergence of the distribution of the simulation results (Veregin, 1997; Lindsay, 2006). Thus the SMA approach was adopted in this paper. The SMA approach is based on the fact that convolving an uncorrelated random field with a low-pass filter increases spatial structure within the field (Wechsler, 2000; Gatziolis and Fried, 2004; Oksanen and Sarjakoski, 2005). Wechsler (2000) was one of the first researchers to apply spatial filtering to stochastic simulation applications. Gatziolis and Fried (2004) demonstrated that the degree of autocorrelation and the distance beyond which two points are unlikely to be dependent in an error field (i.e. the range of the semivariogram) are determined by the size of the low-pass filter used to generate the field. Process convolution (Oksanen and Sarjakoski, 2005) is a special case of the SMA approach, whereby the weights of the convolution kernel (i.e. the low-pass filter) are set in such a way that the resulting error field possesses spatial characteristics that closely approximate an *a priori* correlogram (directly analogous to the semivariogram). Of course, this implies that the spatial structure of elevation error is known *a priori*, which is often not the case.

DOI: 10.1002/hyp

STUDY AREAS

Three basins, representing a range of sizes and physiographic settings, were selected for this study. Newlands Beck (Figures 1a and 1b) is a 24 km^2 basin located in the Lake District of northern England. It is the most mountainous of the three river basins, with a catchment relief of approximately 760 m. The Newlands basin is characterized by wide, glacially-eroded U-shaped valleys, with well defined ridges and small interfluves. The bedrock geology is the mudstones and sandstones of the Ordovician Skiddaw group and land use in the valley is rough grazing on the valley sides with some improved pasture in the valley bottom.

The River Ashop (Figures 1c and 1d), situated within the Peak District National Park, UK, is a 44 km^2 basin (430 m relief) which flows into Ladybower Reservoir. The river is dendritic in pattern with wide interfluves

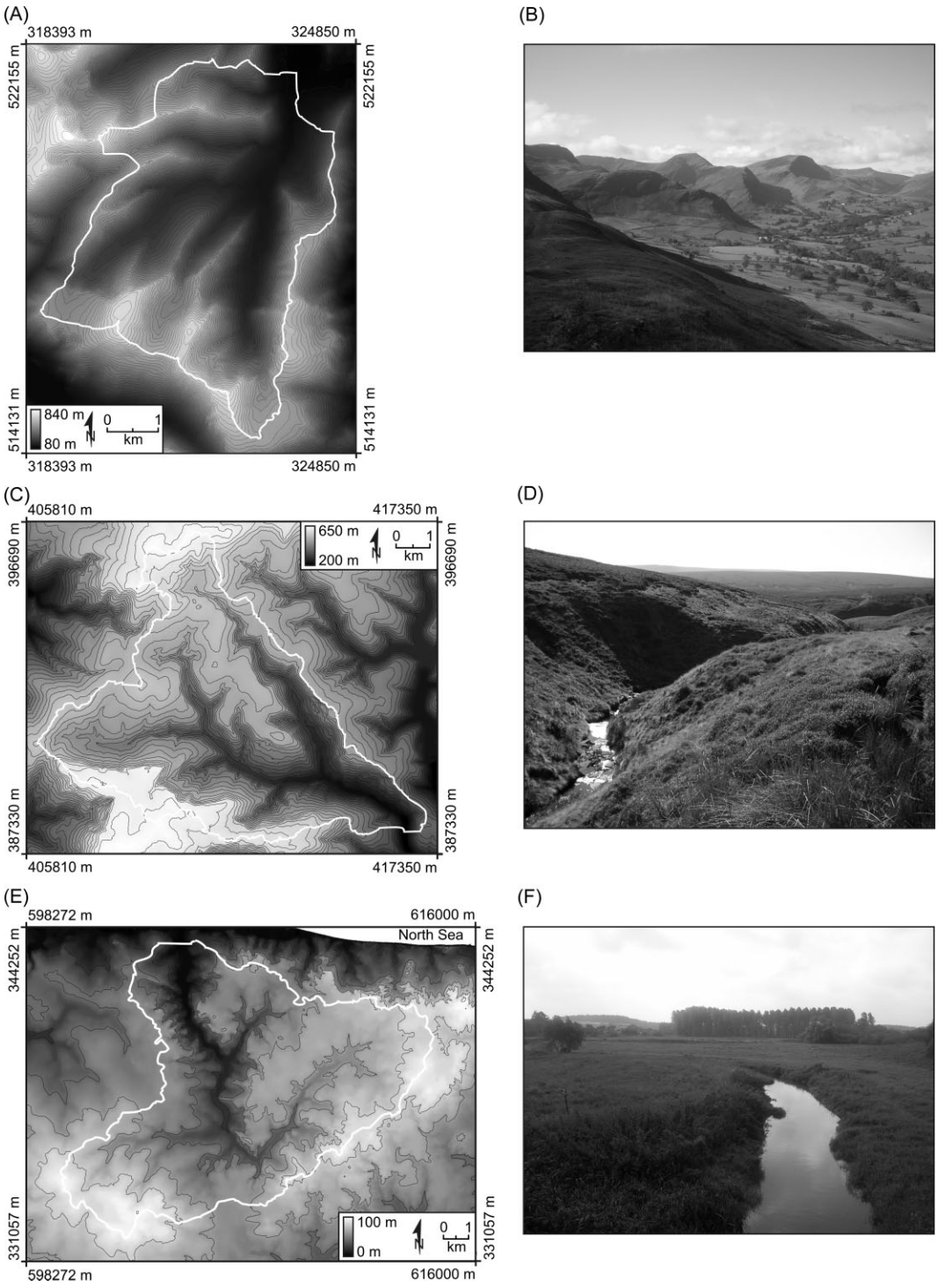

Figure 1. (a) Newlands Beck map and (b) photograph, (c) the River Ashop map and (d) photograph, and (e) the River Glaven map and (f) photograph. DEMs are displayed as greyscale images set within the maps. Contour lines are thin black lines (20 m interval) and watershed divides are thick white lines. Map coordinates are based on the OS National Grid

DOI: 10.1002/hyp

which, in many locations, are dissected by extensive gully networks actively eroding the basin's headwater peatlands. The Bleaklow and Kinder upland areas occupy the basin's northern and southern boundaries respectively. The area is predominantly underlain by inter-bedded coarse-grained sandstone (Millstone Grit) and shale. The dominant land use is rough grazing and management of the moor for grouse shooting with some coniferous plantation forestry in the lower part of the catchment.

The River Glaven (Figures 1e and 1f) located in Norfolk, England, is the flattest of the three study basins, with only 100 m of relief. Runoff from this coastal basin enters the North Sea behind Blakeney spit, draining an area of nearly 93 km^2. The regional geology consists of a complex sequence of glacial, fluvial and marine deposits overlying chalk bedrock. The river flows over a chalk bed in parts of the lower catchment. The major land use is arable agriculture, but there are extensive areas of reed bed in the lower valley and scattered woodland across the valley. It should be noted that the chalky subsurface geology of the Glaven basin may result in substantial losses of stream flow, making the use of network morphometrics based approaches to hydrological modelling difficult. Regardless, the focus of the present paper was not the accurate quantification of stream flow, but rather in evaluating uncertainty in estimates of stream morphometrics. The only relevant characteristic of the local bedrock, therefore, is its potential for affecting stream network form and basin relief.

METHODS

Data

The British Ordinance Survey's (BOS) Land-Form PROFILE™ DEMs were acquired for each of the three study basins (Figure 1). These DEMs possessed 10 m grid resolutions. Land-Form PROFILE™ DEMs are interpolated from 1 : 10 000 contour and spot height data. The metadata associated with the terrain models indicate that the RMSE of the original contour data from which the DEMs were generated is 1·8 m, based on an estimate of the national average (Ordinance Survey, 2001). The height accuracy of any point in a Land-Form Profile DEM is equal to or better than half the contour interval of the primary contour data, that is ±5 m. This accuracy assessment was determined using high accuracy surveying techniques to compare the heights of points along contours extracted from maps and the actual ground position. No information is published on the spatial characteristics of error in Land-Form Profile DEMs, as is frequently the case with published terrain data (Wechsler, 2003). There is also little published data on the nature of the interpolation routine used to generate the DEMs, although it is known that edge-matching procedures were followed to minimize the occurrence of artefacts along tile edges. Each of the three study DEMs were created by mosaicing several 5 km × 5 km tiles using a nearest neighbour re-sampling algorithm. All DEM processing and analysis was conducted using Terrain Analysis System (Lindsay, 2005), a freely-available geographical information system specifically designed for terrain analysis and simulation modelling.

Simulations

The heuristic approach to stochastic simulation (i.e. an unconditional simulation) was adopted in this study because higher accuracy elevation data were unavailable and the metadata associated with the Land-Form PROFILE™ DEMs did not include information about the spatial nature of elevation error. Random fields were created by first assigning each cell in a grid a random value between 0 and 1. This produces a spatially uncorrelated random field (i.e. white noise). While information about the spatial structure of error was unavailable, it is generally accepted that elevation error has a high degree of spatial autocorrelation because both the DEM and the actual surface are smooth (Hunter and Goodchild, 1997). It can therefore be inferred that the error surface is also spatially autocorrelated and does not contain spikes or pits, i.e. large changes in value over short distances. The autocorrelation of the initial spatially uncorrelated random field was increased by convolution with a low-pass filter, i.e. the SMA technique.

A range of filter sizes was used in this study. Random fields were created using circular Gaussian low-pass filters possessing diameters of 50, 150 and 310 m (the three filters had diameters of 5, 15 and 31 grid cells, respectively). These values were selected as they represented a wide range in values, with the largest filter dimension nearly equal to the average hillslope length at each site. In total, nine unconditional simulations were carried out (i.e. three sites × three filter dimensions) and several network morphometrics were measured from each stream network extracted from the terrain realizations. Figure 2 shows examples of the spatial and statistical characteristics of error fields generated using the procedure described above.

While filtering a random field does enhance the spatial autocorrelation of the field, it also alters statistical properties, particularly the error magnitude. Gatziolis and Fried (2004) multiplied the resulting error field by a constant (related to the filter size) to re-scale the statistical distribution to the desired error magnitude. In this study, histogram matching was used to force the spatially autocorrelated error fields to have Gaussian statistical distributions with means of 0 m and standard deviations of 1·8 m (i.e. the published estimate for the RMSE of the DEMs). This approach was more flexible as it meant that the initial uncorrelated error field did not need to have the same statistical distribution as the desired result and, although error fields in this study had Gaussian distributions, histogram matching allowed for the potential to create error fields with any desired statistical distribution shape. This would become relevant if future work were to reveal that the error statistical distribution could not be adequately approximated by a Gaussian distribution.

DOI: 10.1002/hyp

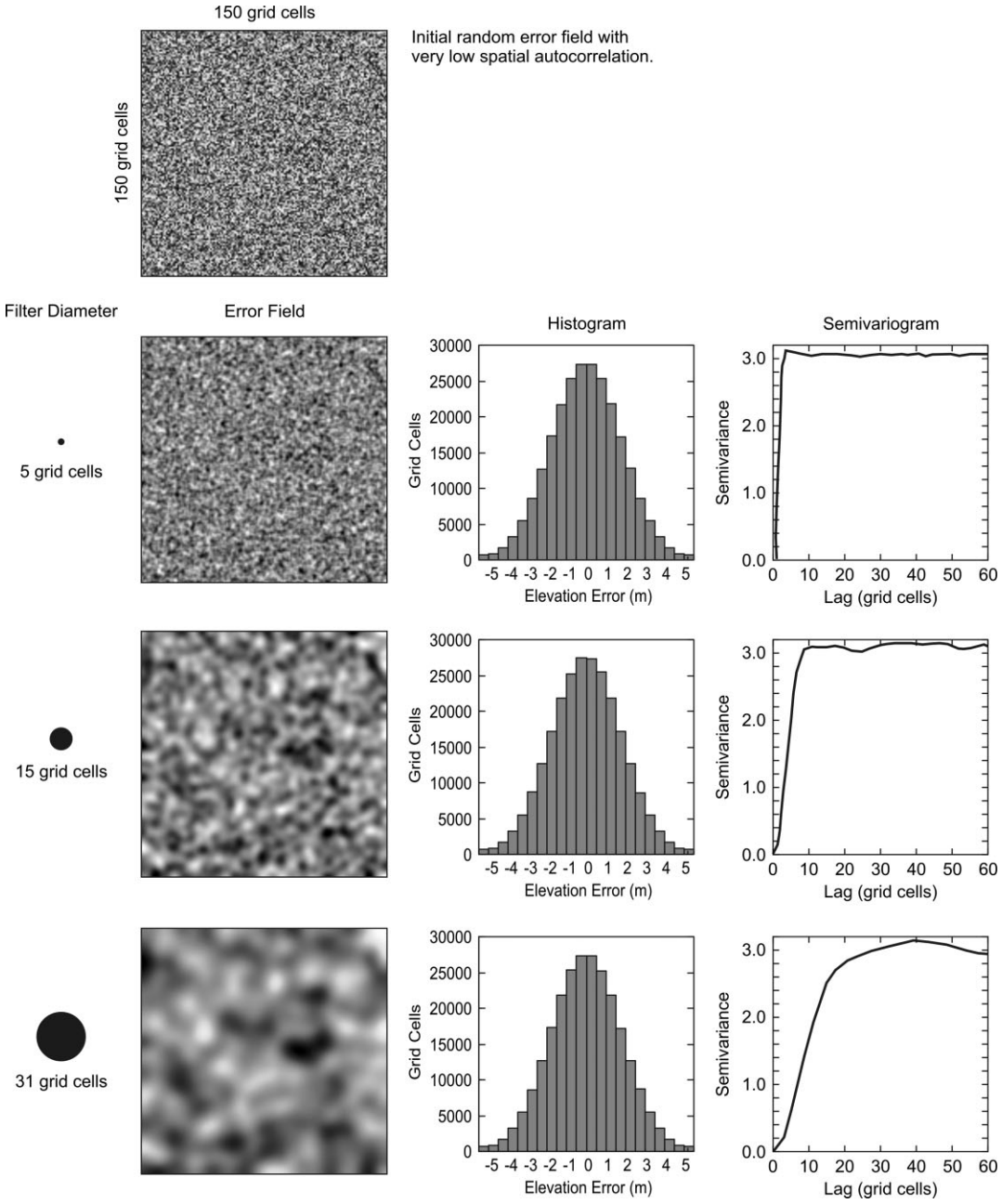

Figure 2. The effects of filtering a small (150 × 150) uncorrelated random field using various sized Gaussian filters on the spatial and statistical properties of the resulting error field. Notice that the histograms of each error field are almost identical because a histogram matching procedure was used post-filtering to force error fields to have the desired statistical distribution

Each terrain realization was hydrologically conditioned (i.e. depressions and flat areas were removed) to allow a stream network to be extracted and the appropriate network indices to be measured. The Planchon and Darboux (2001) method was used for DEM pre-processing because its high efficiency was suited to the iterative approach of stochastic simulation. Stream networks were extracted using the O'Callaghan and Mark (1984) steepest descent, eight-direction (D8) algorithm, in which streams were identified as grid cells possessing contributing area values exceeding a threshold value for channel initiation. A threshold of 5000 m^2 was used in all nine simulations. This value was selected because it provided realistic networks for each of the three basins. It is possible that a different threshold may have yielded slightly different results; however, the effect of the contributing area threshold was not the focus of this paper (for more on this topic see Gandolfi and Bischetti, 1997). The D8 flow routing algorithm was used because the network analysis algorithms, i.e. the algorithms that derived each of the network morphometrics, required single-cell wide streams and used the D8 method to navigate through networks. Clearly the choice of flow algorithm could potentially affect the character of the extracted channel network. Lindsay (2006) demonstrated, however, that while different flow routing algorithms may produce significantly different patterns of upslope contributing area, extracted stream networks are generally very similar. This

DOI: 10.1002/hyp

observation is linked to the fact that most channels occur in convergent topography and the major differences in contributing area patterns produced by available flow algorithms occur on divergent hillslopes.

Each simulation ended after 500 iterations. Lindsay (2006) argued that it is preferable to use a stopping condition based on the stability of the frequency distribution that results from the simulation, rather than a pre-determined number of iterations. A stability-based stopping condition was not used in this study because it was impractical to evaluate the stability of 11 frequency distributions (i.e. one for each morphometric measured from each network realization) simultaneously. Testing of several of the distributions showed that a sufficient degree of stability had been achieved after 500 iterations.

Network morphometrics

Table I identifies the 11 morphometrics that were measured for each realization of the drainage networks of the three study basins. Drainage density was not included in this study as a constant contributing area threshold was used for network extraction. It can therefore be expected that any variation in drainage density is actually a result of variation in the estimated basin area. Although basin area was included in this study, it is clearly not a parameter of the stream network *per se* but it is related to network extent.

Basin boundaries were delineated for each realization, i.e. 500 times for each simulation. Therefore, in determining the DEM extent of the three study elevation models, the likely maximum extent of the probable watershed was considered, i.e. an ample buffer was used to ensure that the 'probable drainage basin' would not intersect the edge of the DEM.

RESULTS

Effects on simple network indices

Although estimates of stream order Ω for the River Ashop were found to be resilient to elevation error, tests did show some uncertainty in Ω estimates for the Newlands and Glaven basins (Figure 3). (Note that the sum of probabilities of Ω values associated with a basin and filter size in Figure 3 total one.) The simulation results for Newlands Beck and the River Glaven showed more sensitivity to the spatial structure of elevation error than was observed for the Ashop basin, i.e. there was sensitivity to variation in the filter size used to generate the error fields. Nonetheless, estimates of Ω were constrained to two values in each basin (4–5, 4–5 and 5–6 for the Newlands, Ashop and Glaven basins respectively). Therefore, stream order was found to be a robust network index. This finding likely reflects the known insensitivity of stream order to network structure.

Table I. Stream network morphometrics measured from each network realization

Morphometric	Symbol	Definition
Stream order at outlet	Ω	Based on Horton-Strahler ordering scheme.
Bifurcation ratio	R_B	N_{w-1}/N_w, where N is the number of streams of successive orders w.
Length ratio	R_L	L_w/L_{w-1}, where L is the mean stream length of successive orders w.
Area ratio	R_A	A_w/A_{w-1}, where A is the mean total contributing area of successive orders w.
Slope ratio	R_S	S_{w-1}/S_w, where S is the mean channel slope of successive orders w.
Basin area	A	Area contributing runoff to the basin outlet.
Stream magnitude at outlet	M	Number of source links within the channel network.
Network diameter	D	Maximum link distance within the channel network.
θ	θ	GIUH parameter describing the geomorphological control on flood magnitude, defined in Equation (3).
k	k	GIUH parameter describing the geomorphological control on flood magnitude, defined in Equation (4).
Network width	$N(x)$	Number of channels at successive distances x from the basin outlet.

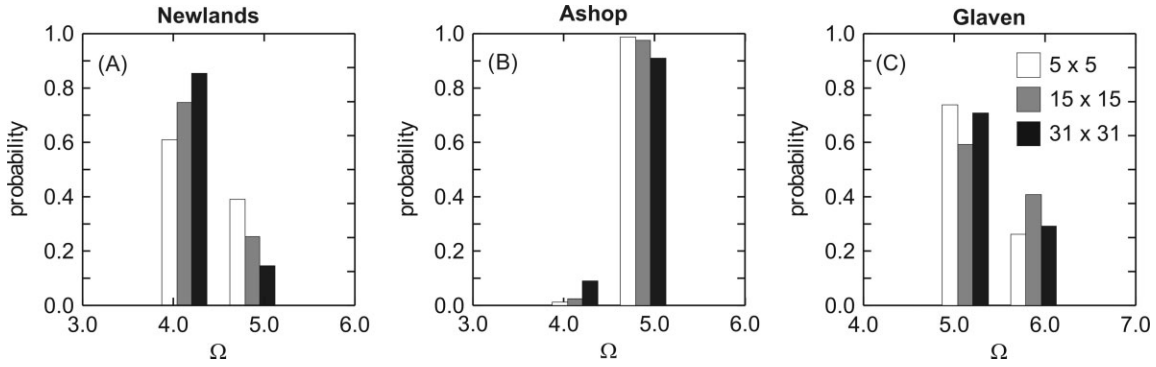

Figure 3. Simulated estimates of Ω for the (a) Newlands, (b) Ashop and (c) Glaven basins. Bar colours refer to the different sized filters used to add spatial autocorrelation to error fields

DOI: 10.1002/hyp

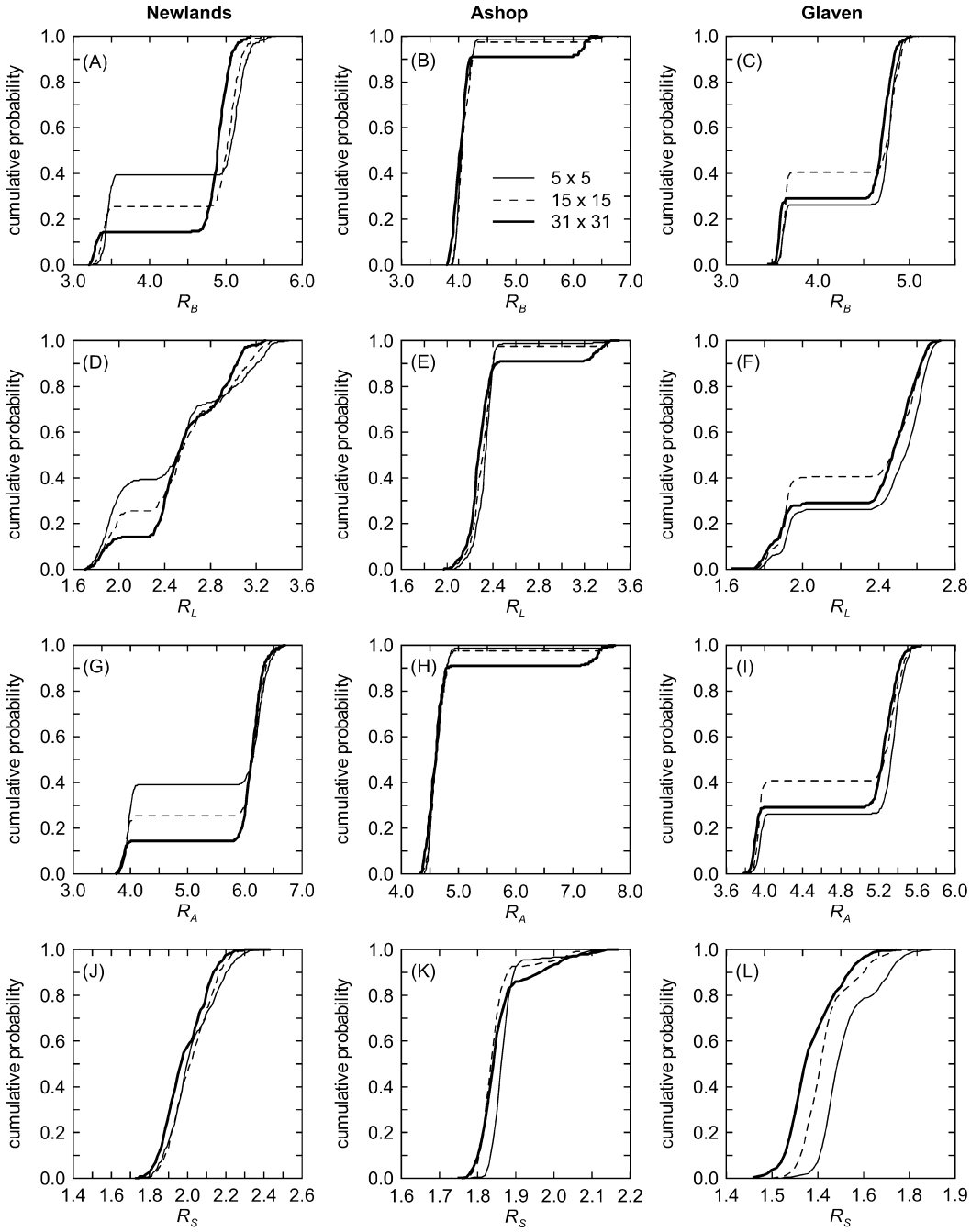

Figure 4. Cumulative distributions of 500 simulated estimates of the Horton ratios R_B, R_L, R_A and R_S for the Newlands, Ashop and Glaven basins

Figure 4 presents the distributions of Horton ratios for the simulations. These data are presented as cumulative distribution functions (cdf) rather than probability density functions (pdf). Cumulative plots are useful for clearly illustrating several distributions of ratio-level data on a single plot. Unimodal distributions tend to have S-shaped cdfs while multimodal distributions have stepped cdfs. Steep parts of the cumulative distribution correspond to peaks in the pdf and flatter parts of the curve correspond to tails or values with no probability of occurrence.

The distributions of estimated R_B, R_L and R_A values were each found to be bimodal (Figure 4), except for the distribution of R_L for Newlands Beck (Figure 4d), which possessed three relatively flat peaks. The distributions of estimated R_S values were unimodal (Figures 4j–l). None of the simulation results for the ratios demonstrated any discernable trend with respect to the differences in basin relief or area. The Horton ratio estimates for the River Ashop did, however, show less overall sensitivity to the spatial properties of error fields than the other two basins. Because of the multimodal characteristics of most of the Horton ratio distributions, it would have been inappropriate to quantify the degree of uncertainty in value assignment using a measure of spread, such as the standard deviation or the inter-quartile range. However, the range of possible estimates for each test spanned the entire range of values of the ratios typically observed for natural rivers (3–5, 1·5–3, 3–6 and 1–2·5 for R_B, R_L, R_A

DOI: 10.1002/hyp

and R_S, respectively). In many instances, the estimates of the ratios extended well beyond their natural ranges. For several simulation tests, it was as probable to observe relatively low values of R_B, R_L and R_A as it was to observe a high value for different realizations of the same channel network.

Figure 5 shows the distributions of basin area estimated values for all nine tests (Figures 5a, 5c and 5e). These data show that the degree of spatial autocorrelation in the elevation error field did not affect the distribution of estimated values substantially, except perhaps for the River Ashop. Figure 5 also presents images of the probability of grid cells being classified as part of the basin for the three 15×15 filter tests (Figures 5b, 5d and 5f). These images clearly show that, as might be expected, the uncertainty in boundary definition is greatest along flatter headwater regions. At least for the three study basins examined here, the results demonstrate that this uncertainty in basin boundary definition can lead to substantial uncertainty in estimates of basin area. The coefficients of variation for estimates of A for the 15×15 filter tests were 0·7%, 1·2% and 1·3% for the Newlands, Ashop and Glaven

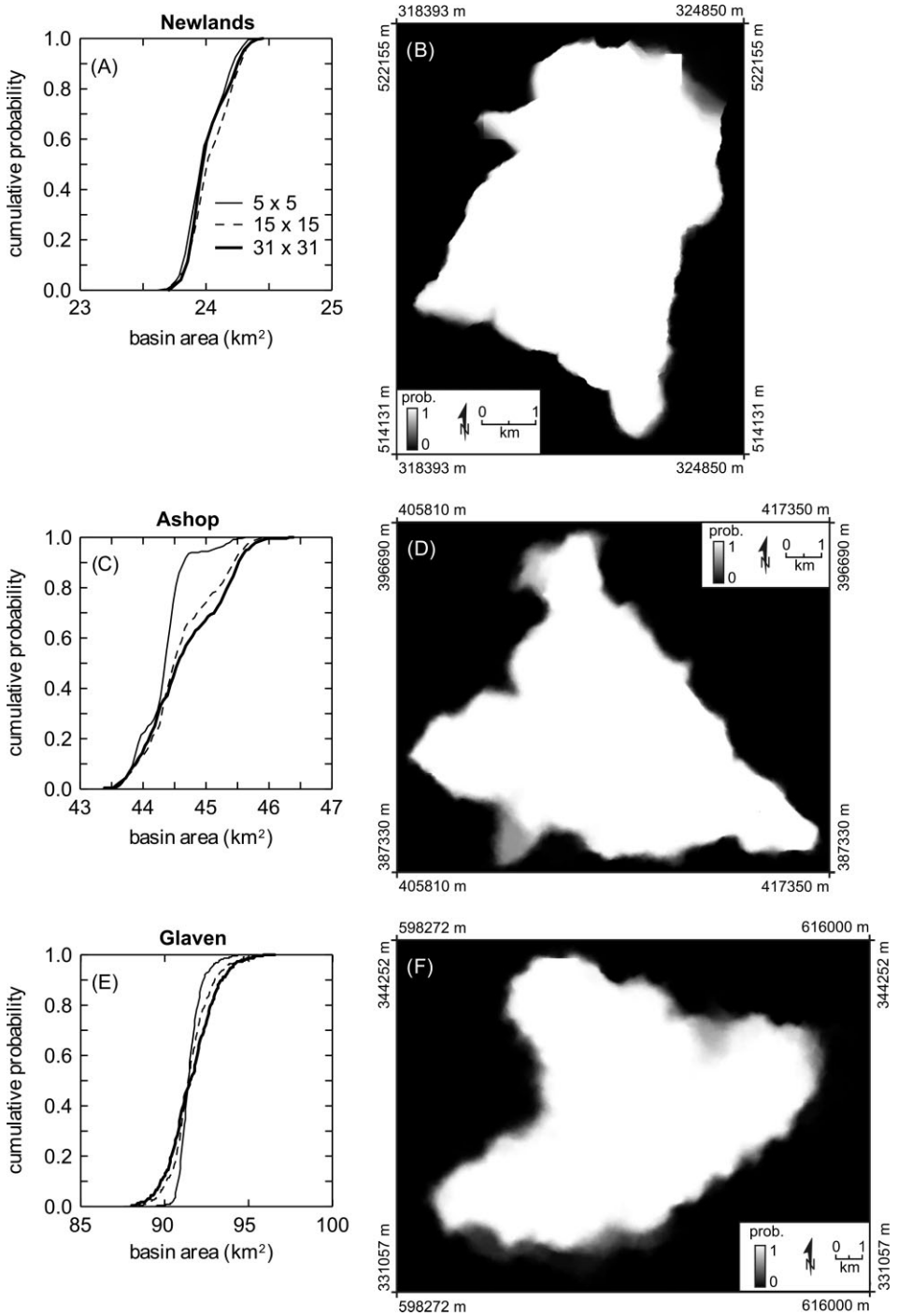

Figure 5. (a), (c) and (e) Cumulative distributions of 500 estimated values of A and (b), (d) and (f) corresponding images of the probability of grid cells belonging to the basin for each of the three study basins

DOI: 10.1002/hyp

basins, respectively, which also shows that the degree of uncertainty in estimates of A resulting from DEM error increases with basin relief. The maximum estimates of A were found to be 3·6%, 5·9% and 9·1% larger than the minimum estimates for the Newlands, Ashop and Glaven basins, respectively. Certainly for the larger Glaven basin, this value represents a significant uncertainty in the overall basin water balance.

Unlike most of the Horton ratio distributions, the distributions for network magnitude and diameter were found to be unimodal (Figure 6). Therefore, for each test and in each of the three basins, one value of M and D was more probable than any other. There was, however, substantial uncertainty in these two topology-based morphometrics. The distributions of M and D demonstrated that a wide range of estimated values were possible given the degree of uncertainty in the DEM (e.g. estimates of M for the River Glaven differed by up to 78 within a single simulation test). Furthermore, the uncertainties in M and D were inversely related to basin area. For instance, the estimates of M for Newlands Beck, the River Ashop and the River Glaven (smallest to largest) had coefficients of variation 4·1%, 2·9% and 2·4%, respectively (15 × 15 filter test).

There was also considerably greater sensitivity in M and D to the spatial structure of elevation error than was observed for the indices based on stream order (Figure 6). Although the spread of the M and D distributions was not influenced by the filter size, the distributions were clearly shifted. It is evident that as the spatial extent of autocorrelation increased, the total number of source links within each stream network and the network diameter decreased.

Effects on indices used in modelling runoff response

Figure 7 shows the simulation results for the parameters related to runoff response, including the GIUH parameters θ, k and $N(x)$. The resulting distributions for the GIUH parameters were multimodal, although there was one highly dominant peak for several of the simulation tests. Sensitivity to elevation error was lowest in both parameters for the River Ashop (Figures 7b and 7e) and much higher in the Newlands and Glaven basins. Like most of the stream-order based indices, neither of the GIUH parameters showed significant sensitivity to the spatial properties of the error field. Thus, while the form of the GIUH is clearly impacted by the statistical distribution of elevation errors, it is less affected by the degree of spatial autocorrelation in topographic uncertainty.

The simulations yielded a distribution of estimates of the number of channel links for each 1 km interval along the stream network, i.e. $N(x)$. Figures 7g–i show the 5th and 95th percentiles of these distributions, thereby indicating the degree of uncertainty in the shape of the network width function (90% of the estimated values fall between these lines). Each simulation test revealed a significant separation between the 5th and 95th percentile lines. The average separation was 4·4, 5·7 and 8·0 channels for the Newlands, Ashop and Glaven basins, respectively. Maximum separations were at least double these figures. Therefore, there can be little confidence in the estimated value of network width at any given distance upstream. The uncertainty in $N(x)$ appeared to be inversely related to basin relief (or directly proportional to basin size), with the River Glaven experiencing the greatest degree of uncertainty in the function's shape. Additionally, the separation between the 5th and 95th

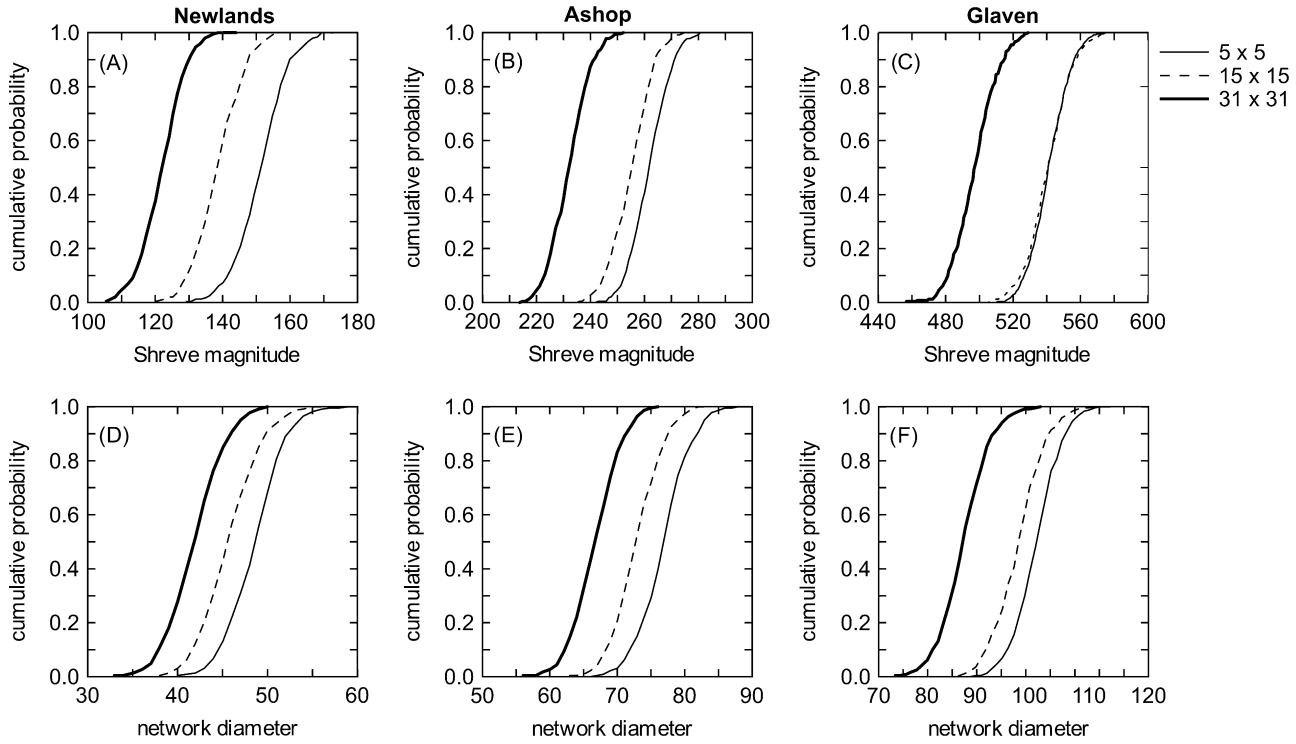

Figure 6. Cumulative distributions of 500 simulated estimates of the topological morphometrics M and D for the study basins

DOI: 10.1002/hyp

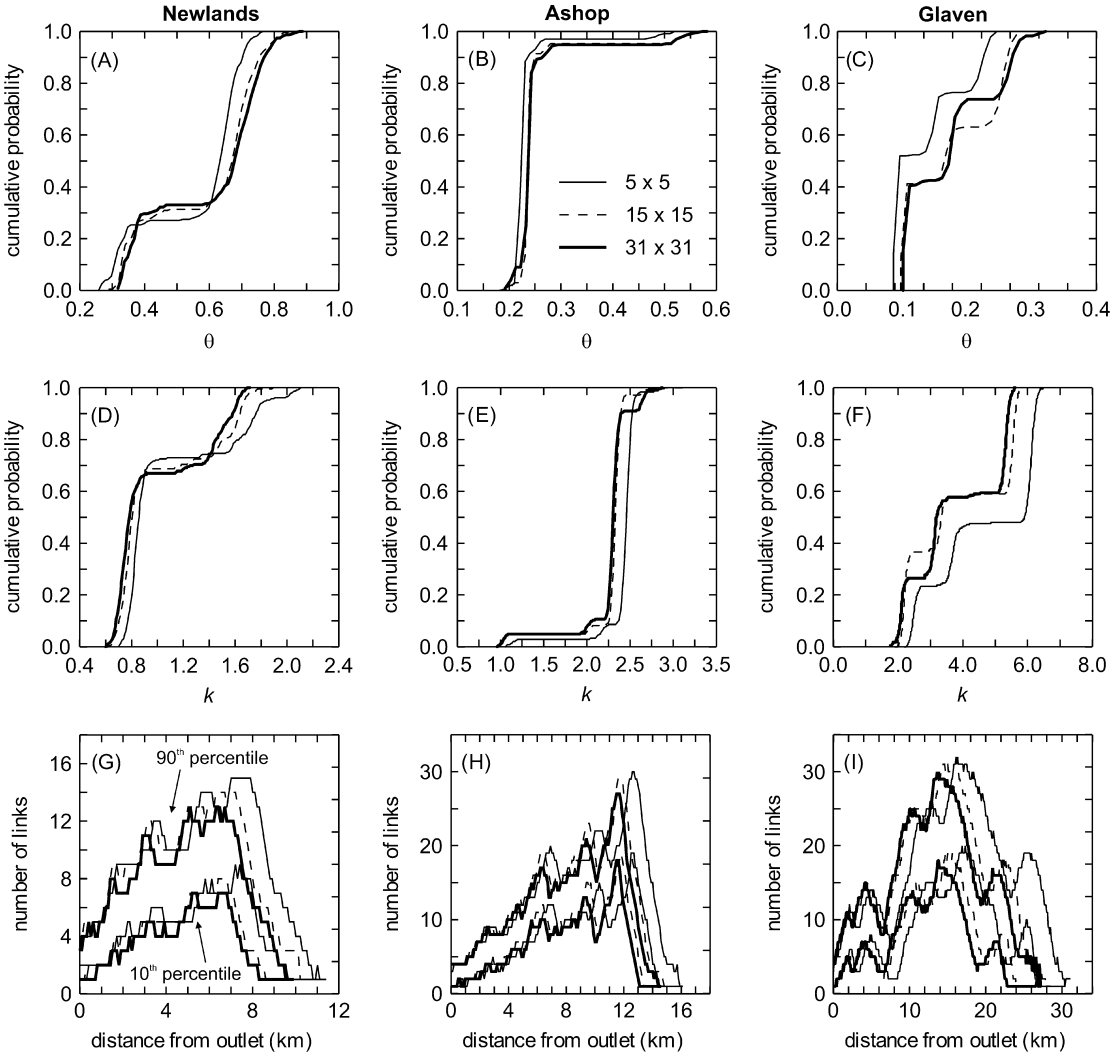

Figure 7. Cumulative distributions of 500 simulated estimates of the hydrological response morphometrics θ, k and $N(x)$ for the study basins

percentile lines generally increased with distance from the outlet (Figures 7g–i). Much of the error in $N(x)$ possibly results from uncertainty in the number and distribution of source links, which were shown to be particularly sensitive to elevation error (Figures 6a–c). This may also explain why there was less uncertainty in $N(x)$ at shorter distances from the outlet, since source links are generally more numerous in the upper, distant portions of basins.

Greater spatial structure within error fields compressed $N(x)$ (Figures 7g–i), effectively shortening the flow-lengths without modifying network topological structure. This occurred because error fields with a high degree of spatial autocorrelation are smooth surfaces, and flow-paths over smoother surfaces meander less (i.e. they are more direct). Thus, varying the filter size used to create the error fields in the simulations affected the estimated value of network width without modifying the overall shape of the function.

DISCUSSION

There is a link between the bimodal distributions of several of the Horton ratios and uncertainty in estimates of Ω for a particular basin. That is, whether a basin is assigned a stream order of 4 or 5 may appear to be a relatively insignificant difference; however, it can have a profound impact on the uncertainty in estimates of Horton ratios. For example, the findings for the Newlands 15 × 15 simulation test showed that 74·6% of the realizations had $\Omega = 4$, while the remaining realizations assigned the basin a stream order of 5 (Figure 3a). This same proportionality can be observed in Figure 4a where the two peaks of the R_B estimates have 25·4% and 74·6% cumulative probabilities, respectively. Evidently, the first R_B peak corresponds to the realizations with $\Omega = 5$ and the second to realizations with $\Omega = 4$, a fact that was also confirmed by examining the results for individual stream network realizations. This relation between the uncertainty in values of Ω and the wide-ranging multimodality in estimates of the Horton ratios can be observed for many of the R_B, R_L and R_A distributions (Figure 4). The relation was found to occur because Horton ratios are estimated by fitting exponential models to data using the least-squares regression method. Because these regression models are fitted to data of relatively small sample sizes, i.e. less than six data

DOI: 10.1002/hyp

points (each point corresponding to a stream order), the equations of the resulting models were found to be highly sensitive to the inclusion of a single extra point. The fact that estimates of R_S did not display bimodal distributions for any of the three study basins probably reflects the fact that the goodness-of-fit of the regression models used to estimate R_S were almost always the poorest of the four Horton ratios (the R^2 of the models fit to the other three Horton ratios are generally 0·98 or greater). Thus, at least in the case of estimates of R_S, the instability in the regression model caused by the small sample size is of the order of the instability caused by the poorer fit of the model to the data.

It has therefore been demonstrated that uncertainty in the assignment of Ω can lead to much greater uncertainty in estimates of Horton ratios (and clearly in the estimates of the GIUH parameters also). The relevant question then becomes: what determines the degree of uncertainty in assignment of Ω for a particular basin? Clearly Ω was estimated for the River Ashop with a much higher degree of confidence than for the other two basins, but what does this reflect about the structure of the Ashop river network or its basin morphology? If a basin is considered to consist of a series of sub-basins, each draining into the main channel of the stream network, then each sub-basin has a degree of uncertainty in its assignment of stream order. It may be, as a hypothetical example, that a particular sub-basin is assigned a stream order of 3 for 80% of the realizations in a simulation test, and a stream order of 4 for the remaining 20% of the realizations. If the main channel of the stream network at the outlet of the sub-basin has a stream order assignment of 5 or 6, taking into account its own uncertainty, then the probability $p_{\Delta SO}$ of the outlet of the sub-basin being an order-changing bifurcation in the network is zero. Therefore, the uncertainty in the assignment of stream order for the hypothetical sub-basin would not affect the estimate of Ω at the basin outlet. If the $p_{\Delta SO}$ of a sub-basin outlet draining into the main channel is either very low or very high, the effect on the uncertainty in the assignment of Ω will be small. However, if for some significant proportion of the realizations in a simulation test the estimated stream order of the sub-basin is equal to that of the main channel, then $0 > p_{\Delta SO} > 1$ and there would be some resulting uncertainty in the assignment of Ω. Clearly, any network can be expected to possess numerous bifurcations with $0 > p_{\Delta SO} > 1$, particularly in low-order tributaries. The effect of such a bifurcation on uncertainty in Ω is eliminated if a downstream bifurcation has either $p_{\Delta SO} \approx 0$ or $p_{\Delta SO} \approx 1$. Therefore, it is only bifurcations draining into the main channel that are likely to affect uncertainty in Ω.

Both the Newlands and Glaven stream networks were found to possess bifurcations draining into their main channels with $0 > p_{\Delta SO} > 1$, which were caused by 'stream captures' further upstream of relatively small catchment areas draining to low-order streams. By comparison, most of the main channel bifurcations in the Ashop river network either had $p_{\Delta SO} \approx 0$ or $p_{\Delta SO} \approx 1$, resulting in considerably more stable estimates of Ω and the Horton ratios. This stable condition is likely to be common to long and narrow basins (i.e. elongated stream networks) in which relatively small sub-basins enter the main channel, which is of significantly higher stream order.

The topological morphometrics M and D were greatly affected by elevation error and, unlike most of the indices based on stream order, demonstrated extreme sensitivity to the degree of spatial autocorrelation in elevation error. Thus, without knowing something about the magnitude of error and the spatial autocorrelation structure of the elevation error in a DEM, it is difficult to have confidence in the estimates of these DEM-extracted indices. The fact that a greater degree of spatial autocorrelation in elevation error results in substantially lower estimated values of M and D (Figure 6) is an important finding. The reason for this phenomenon can be seen in Figure 8, which displays extracts of two contributing area images,

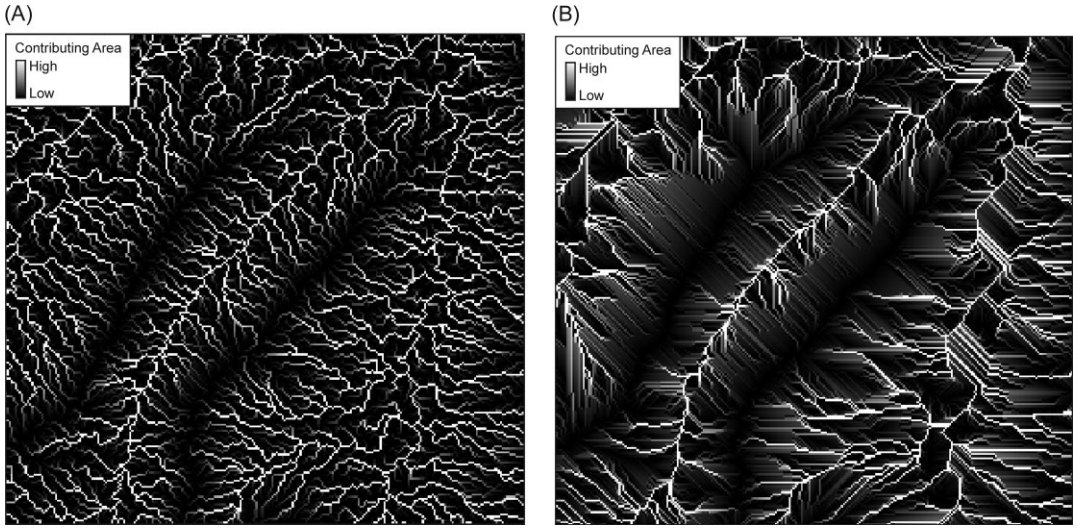

Figure 8. Extracts of contributing area images created during a simulation test with (a) a small degree of spatial autocorrelation in the error field (5 × 5 filter) and (b) a higher degree of autocorrelation (31 × 31 filter)

DOI: 10.1002/hyp

one of which was created during a simulation test with a small degree of spatial autocorrelation in the error field and the other with a much higher degree of autocorrelation. It is apparent that elevation error with a high degree of spatial autocorrelation yields contributing area patterns that possess numerous short, parallel flow-paths. This lack of convergent flow on hillslopes has been recognized as a drawback of the D8 flow routing algorithm (Fairfield and Leymarie, 1991). Error with lower autocorrelation yields contributing area patterns with greater flow-path convergence, and therefore a greater number of grid cells with very low and very high (i.e stream cells) contributing area (and more realistic flow-paths as Fairfield and Leymarie's work highlighted). A greater number of stream cells combined with more bifurcating flow paths (i.e. less parallel flow) will result in more stream links and therefore a higher estimate of M. Another consequence of this phenomena is that while basin area estimates are largely unaffected by the spatial properties of elevation error (Figure 5), drainage density estimates are greatly impacted. This phenomenon also explains the tendency for $N(x)$ to be compressed with increased spatial autocorrelation of elevation error (Figure 7). Clearly, the patterns observed in Figure 8 are largely a function of the use of the D8 flow routing algorithm. Nonetheless, it is emphasized that most algorithms for performing stream network analysis tasks require this flow routing method.

The simulation tests showed that a moderate magnitude of elevation error (RMSE = 1·8 m) can result in significant uncertainty in the estimates of network morphometrics. It would be prudent to consider stream order based morphometrics derived from DEM-mapped stream networks as rough estimates, given the range of measured values relative to their expected ranges and their multimodal distributions. Therefore, while automated stream network analysis procedures may be more objective and repeatable than manual methods based on interpreting stream lines on paper maps, they are not necessarily any more accurate. Additional simulation tests that were conducted using a much lower error magnitude (standard deviation of 1 m) also yielded multimodal frequency distributions for estimates of R_B, R_L, R_A, θ and k (Figure 9). In fact, the low error simulation test yielded remarkably similar ranges in observed values of each of the network morphometrics, demonstrating that this issue is relevant even for highly accurate terrain models. Therefore, care should be exercised when interpreting the results of hydrological or geomorphological analyses obtained from DEM-mapped stream networks. This assertion compliments the findings of Gandolfi and Bischetti (1997) and Da Ros and Borga (1997), both of whom found that morphometrics and modelled hydrological response were affected by parameter uncertainty associated with the automated mapping algorithm.

The range in estimated values of θ and k (Figures 7a–f) resulted in significant uncertainty in the shape of the GIUH, particularly in the Newlands and Glaven basins. Interestingly, the estimate of θ, the parameter related to peak magnitude, was very uncertain in the high-relief Newlands basin (Figure 7a), while the value of k, the parameter related to time-to-peak, was similarly uncertain in the low-relief Glaven basin (Figure 7f). This may indicate that it is difficult to estimate both flood magnitude and timing reliably using the GIUH method, except under certain topographic settings or for some optimal basin size or network structure similar to that observed for the River Ashop.

The observation that variation in the spatial properties of error has the effect of compressing $N(x)$ without modifying its general shape (Figure 7) has important implications for the hydrological applications of the width function. Models of hydrological response that utilize $N(x)$ normalize the function to total network length (e.g. Da Ros and Borga, 1997). Thus, the observed sensitivity to the spatial structure of the elevation error field is unlikely to affect models that use the width function. It should be emphasized, however, that the uncertainty in the shape of $N(x)$ owing to elevation error, regardless of its spatial properties, is enough to cause concern about its application. Furthermore, the uncertainty in the shape of $N(x)$ increases with distance upstream (Figures 7g–i). This error has the greatest effect on the shape of the falling limb of the modelled response function.

CONCLUSIONS

Stochastic simulations revealed the following major findings about the impact of elevation error on the geometric properties of DEM-mapped drainage networks and their modelled hydrological responses:

1. The uncertainty in network morphometrics resulting from moderate to small elevation errors can be very complex. This reflects the intricate way in which surface drainage and stream network structure is affected by error and the use of regression analysis in estimating indices. In particular, the presence of sub-basins draining into the main channel that have moderate probabilities of being order-changing bifurcations was found to cause multimodal distributions for estimates of the indices involving stream order, i.e. two or more estimated values were found to be highly likely. The fact that these preferential estimates can be very wide ranging is most troubling. Thus, often there can be little confidence in the values of stream-order based morphometrics derived from DEMs, even if the DEMs possess relatively small errors. The findings suggest, however, that if a stream network is elongated, with relatively small sub-basins entering the main channel which is of significantly higher stream order, estimates of stream-order based indices can be reliable.
2. Link-based network morphometrics, such as stream magnitude and network diameter, were found to be highly sensitive to elevation error and its spatial characteristics. This reflected the difficulty in using

DOI: 10.1002/hyp

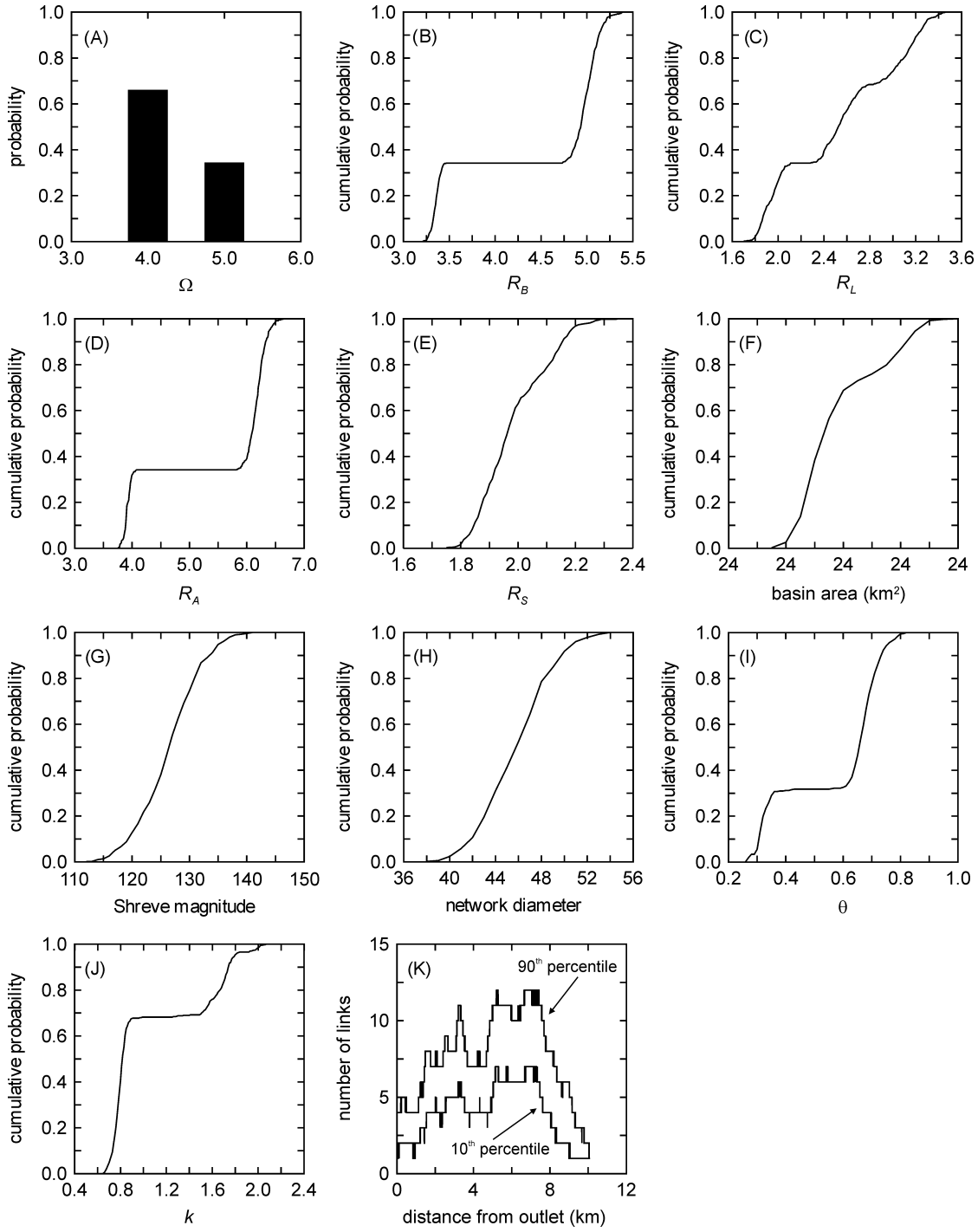

Figure 9. Distributions of network morphometrics for Newlands Beck derived from a simulation test using 1 m standard deviation of elevation error and a 5 × 5 filter to enhance spatial autocorrelation

automated procedures to map source channels and other low-magnitude links. In general, network morphometrics are heavily influenced by the number of source channels, which is very sensitive to error. This research, in the same way as that of previous workers, shows that automated mapping algorithms are particularly strained to accurately identify low-order streams. This issue may be partially resolved by using high-resolution terrain data (e.g. LIght Detection And Ranging, or LiDAR) in combination with morphological-based channel mapping techniques, instead of methods that are based on identifying channel heads which are currently more popular.

3. For certain stream network shapes (i.e. elongated networks), such as the River Ashop, the parameters expressing the geomorphological control over the shape of the GIUH can be quite insensitive to elevation error. Nonetheless, uncertainty in flood magnitude and timing parameters can be significant under other conditions. It appears that if the topological characteristics of a stream network or the physiographic properties of a basin result in an estimate of flood magnitude that

DOI: 10.1002/hyp

is insensitive to elevation error, the estimate of timing demonstrates high sensitivity, and vice versa. This can lead to substantial uncertainty in the shape of the unit hydrograph.

4. Network width functions derived from stream networks that are mapped from DEMs are greatly affected by elevation error, and in particular, its spatial properties. Increasing the degree of spatial autocorrelation in elevation error decreases measured flow-path lengths, effectively compressing the width function. This may not affect hydrological models that use the width function substantially because the function is commonly normalized for total stream length. Nevertheless, error in estimates of network width increased significantly in the upstream direction. This was thought to be due to the difficulty in mapping source channels and other low-magnitude streams. The higher error in estimates of network width at greater distances from the outlet results in greater uncertainty in the falling limb of the response hydrograph.
5. It is evident that more work is needed to characterize the actual spatial nature of elevation error in DEMs, particularly because of the demonstrated sensitivity of several network morphometrics to the spatial properties of this error.

ACKNOWLEDGEMENTS

The authors appreciate the insightful comments of the anonymous reviewers which have served to greatly strengthen this paper.

REFERENCES

Beven KJ. 2000. *Rainfall-Runoff Modelling: The Primer*. John Wiley & Sons: Chichester; 360 pp.

Burrough PA, McDonnell RA. 1998. *Principles of geographical information systems*. Oxford University Press: New York; 333 pp.

Carlisle BH, Heywood DI. 1996. The accuracy of a mountain DEM: Research in Snowdonia, North Wales, UK, Bax D (ed.). In *Proceedings of the 4th International Symposium on High Mountain Remote Sensing Cartography*, Karlstad, Sweden, University of Karlstad, Natural Sciences/Technology Research Report No 97:03: 71–86. http://www.kfunigraz.ac.at/geowww/hmrsc/proceedings4.htm [accessed 10 July 2007].

Carr JR. 2002. *Data Visualization in the Geosciences*. Prentice Hall: London; 267 pp.

Cressie N, Pavlicová M. 2002. Calibrated spatial moving average simulations. *Statistical Modelling: An International Journal* **2**(4): 267–279.

Da Ros D, Borga M. 1997. Use of digital elevation model data for the derivation of the geomorphological instantaneous unit hydrograph. *Hydrological Processes* **11**: 13–33.

Deutsch CV, Journel AG. 1998. *GSLIB Geostatistical Software Library and User's Guide*. Oxford University Press: New York; 369 pp.

Endreny TA, Wood EF. 2001. Representing elevation uncertainty in runoff modelling and flowpath mapping. *Hydrological Processes* **15**: 2223–2236.

Endreny TA, Wood EF, Lettenmaier DP. 2000. Satellite-derived elevation model accuracy: hydrological modelling requirements. *Hydrological Processes* **14**(2): 177–194.

Fairfield J, Leymarie P. 1991. Drainage networks from grid digital elevation models. *Water Resources Research* **27**(5): 709–717.

Fisher PF. 1991. First experiments in viewshed uncertainty: the accuracy of the viewable area. *Photogrammetric Engineering and Remote Sensing* **57**: 1321–1327.

Fisher P. 1998. Improved modelling of elevation error with geostatistics. *Geoinformatica* **2**: 215–233.

Gandolfi C, Bischetti GB. 1997. Influence of the drainage network identification method on geomorphological properties and hydrological response. *Hydrological Processes* **11**: 353–375.

Gandolfi C, Bischetti GB, Whelan MJ. 1999. A simple triangular approximation of the area function for the calculation of network hydrological response. *Hydrological Processes* **13**(17): 2639–2653.

Gatziolis D, Fried JS. 2004. Adding Gaussian noise to inaccurate digital elevation models improves fidelity of derived drainage networks. *Water Resources Research* **40**: W02508. DOI:10·1029/2002WR01735.

Goodchild MF, Sun G, Yang S. 1992. Development and test of an error model for categorical data. *International Journal of Geographical Information Systems* **6**(2): 87–104.

Goovaerts P. 1997. *Geostatistics for Natural Resources Evaluation*. Oxford University Press: New York; 483 pp.

Gupta VJ, Messa O. 1988. Runoff generation and hydrologic response via channel network geomorphology—recent progress and open problems. *Journal of Hydrology* **102**: 3–28.

Gyasi–Agyei Y, Willgoose G, De Troch F. 1995. Effects of vertical resolution and map scale of digital elevation models on geomorphological parameters used in hydrology. *Hydrological Processes* **9**: 363–382.

Heine RA, Lant CL, Sengupta RR. 2004. Development and comparison of approaches for automated mapping of stream channel networks. *Annals of the Association of American Geographers* **94**(3): 477–490.

Heuvelink GBM. 1998. *Error Propagation in Environmental Modelling with GIS*. Taylor & Francis: London.

Horton RE. 1945. Erosional development of streams and their drainage basins: hydrophysical approach to quantitative morphology. *Geological Society of America Bulletin* **56**: 275–370.

Horton RE. 1932. Drainage basin characteristics. *Eos Transactions of the American Geophysical Union* **13**: 350–361.

Hunter GJ, Goodchild MF. 1997. Modeling the uncertainty of slope and aspect estimates derived from spatial databases. *Geographical Analysis* **29**: 35–49.

Kenward T, Lettenmaier DP, Wood EF, Fielding E. 2000. Effects of digital elevation model accuracy on hydrologic predictions. *Remote Sensing of Environment* **74**(3): 432–444.

Kirkby M. 1976. Test of the random network model and its application to basin hydrology. *Earth Surface Processes* **1**: 197–212.

Knighton D. 1998. *Fluvial Forms and Processes: A New Perspective*. Arnold Publishing: London, 383 pp.

Lee J, Snyder PK, Fisher PF. 1992. Modeling the effect of data errors on feature extraction from digital elevation models. *Photogrammetric Engineering and Remote Sensing* **58**: 1461–1467.

Lindsay JB. 2005. The Terrain Analysis System: A tool for hydro-geomorphic applications. *Hydrological Processes* **19**: 1123–1130.

Lindsay JB. 2006. Sensitivity of channel mapping techniques to uncertainty in digital elevation data. *International Journal of Geographical Information Science* **20**(6): 669–692.

McMaster KJ. 2002. Effects of digital elevation model resolution on derived stream network position. *Water Resources Research* **38**: 1042. DOI:10·1029/2000WR000150.

Mark DM. 1984. Automated detection of drainage networks from digital elevation models. *Cartographica* **21**: 168–178.

Mesa OJ, Mifflin ER. 1986. On the relative role of hillslope and network geometry in hydrologic response. In *Scale Problems in Hydrology*, Gupta VK, Rodriguez–Iturbe I, Wood EF (eds). Reidel: Dordrecht, 159–184.

Naden PS. 1992. Spatial variability in flood estimation for large catchments: the exploitation of channel network structure. *Hydrological Sciences Journal* **37**: 53–71.

O'Callaghan JF, Mark DM. 1984. The extraction of drainage networks from digital elevation data. *Computer Vision, Graphics, & Image Processing* **28**: 323–344.

Oksanen J. 2006. *Digital Elevation Model Error in Terrain Analysis*. Helsinki University Press: Helsinki, 51 pp.

Oksanen J, Sarjakoski T. 2005. Error propagation analysis of DEM-based drainage basin delineation. *International Journal of Remote Sensing* **26**(14): 3085–3102.

Ordinance Survey. 2001. *Land-Form PROFILE User Guide, v. 4*, http://www.ordnancesurvey.co.uk/oswebsite/products/landformprofile/pdf/profil_w.pdf. Last accessed: September 7, 2005.

Planchon O, Darboux F. 2001. A fast, simple and versatile algorithm to fill the depressions of digital elevation models. *Catena* **46**: 159–176.

Rodriguez–Iturbe I, Valdes JB. 1979. The geomorphic structure of hydrologic response. *Water Resources Research* **15**(6): 1409–1420.

Schumm SA. 1956. Evolution of drainage systems and slopes in Badlands at Perth Ambos, New Jersey. *Geological Society of America Bulletin* **67**: 597–646.

Shreve RL. 1966. Statistical law of stream numbers. *Journal of Geology* **75**: 178–186.

Smart JS. 1978. The analysis of drainage network composition. *Earth Surface Processes and Landforms* **3**: 129–170.

Strahler AN. 1952. Hypsometric (area-altitude) analysis of erosional topography. *Geological Society of America Bulletin* **63**: 1117–1142.

Surkan AJ. 1969. Synthetic hydrographs: Effects of network geometry. *Water Resources Research* **5**(1): 112–128.

Tribe A. 1992. Automated recognition of valley lines and drainage networks from digital elevation models: a review and a new method. *Journal of Hydrology* **139**: 263–293.

Veregin H. 1997. The effects of vertical error in digital elevation models on the determination of flow-path direction. *Cartography and Geographic Information Systems* **24**(2): 67–79.

Walker JP, Willgoose GR. 1999. On the effect of digital elevation model accuracy on hydrology and geomorphology. *Water Resources Research* **35**(7): 2259–2268.

Wechsler S. 2000. *Effects of DEM uncertainty on topographic parameters, DEM scale and terrain evaluation*. Ph.D. dissertation. College of Environmental Science and Forestry, State University of NY, Syracuse.

Wechsler S. 2003. Perceptions of digital elevation model uncertainty by DEM users. *URISA Journal* **15**(2): 57–64.

Wechsler S. 2006. Uncertainties with digital elevation models for hydrological applications: a review. *Hydrology and Earth System Sciences Discussions* **3**: 2343–2384.

Werner C, Smart JS. 1973. Some new methods of topologic classification of channel networks. *Geographical Analysis* **5**: 271–295.

Wharton G. 1994. Progress in the use of drainage network indices for rainfall-runoff modelling and runoff prediction. *Progress in Physical Geography* **18**(4): 539–557.

Wolock DM, Price CV. 1994. Effects of digital elevation model map scale and data resolution on a topography-based watershed model. *Water Resources Research* **30**(11): 3041–3052.

DOI: 10.1002/hyp